Case Studies in Thermal Engineering 53 (2024) 103929

Contents lists available at ScienceDirect

Case Studies in Thermal Engineering

journal homepage: www.elsevier.com/locate/csite

Numerical investigation of the length of a polymer fuel cell on energy production in asymmetric flow and hydrogen production process

Jawed Mustafa [a,*], Saeed Alqaed [a], S. Mohammad Sajadi [b], Hikmet Ş. Aybar [c,d,**]

[a] Mechanical Engineering Department, College of Engineering, Najran University, P.O. Box (1988), Najran, 61441, Saudi Arabia
[b] Department of Nutrition, Cihan University-Erbil, Iraq
[c] Department of Mechanical Engineering, Eastern Mediterranean University, Famagusta, TRNC, via, Mersin 10, Turkey
[d] Department of Medical Research, China Medical University Hospital, China Medical University, Taichung, Taiwan

ARTICLE INFO

Keywords:
Fuel cell
Cell power
Potential electrolyte
Molar hydrogen content

ABSTRACT

In this study, a three-dimensional simulation of fuel cell (FUC) by using FEM is presented. The values of electrolyte potential (EPL), cell power (CPR), hydrogen mole fraction (HMF), water mole fraction (WMF), oxygen mole fraction (OMF), pressure, and rate changes in the channels are determined by changing the voltage from 0.1 to 0.8 V and the length of the hydrogen and oxygen channels (HOC) from 5 to 20 mm. This study is carried out by employing COMSOL software. The results reveal that an enhancement in the length of HOC reduces the amount of CPR. The maximum amount of CPR occurs when the HOC are 5 mm and the voltage is 0.5 V. The minimum amount of CPR corresponds to the channel length of 20 mm and a voltage of 0.8 V. At higher voltages, the use of longer channels increases the EPL. An increment in the voltage significantly reduces the EPL, while increasing the length of the HOC intensifies the EPL. An enhancement in the length of the channel and increasing the applied voltage results in a reduction in the HMF. An increase in the voltage results in a more significant reduction in HMF for larger lengths of the HOC.

1. Introduction

The increasing use of non-renewable fossil resources and their environmental impact has led scientists to explore sustainable energy sources [1,2]. Hydrogen, due to its unique properties, is predicted to play a significant role in future energy production, with experts suggesting that the future belongs to hydrogen and its related technologies [3]. The features that distinguish hydrogen from other fuels are abundant, very little emissions of pollutants, the reversibility of the production cycle, and the reduction of greenhouse effects [4]. Fuel Cell (FUC) technology, where hydrogen undergoes a chemical reaction with oxygen to produce electricity and heat, is considered a promising option for future electric energy production [5]. The advantages of this technology is its high efficiency compared to competing technologies, a wide range of power generation from nanowatts to megawatts, wide applications in various industries, such as electricity, transportation, information and communication, military, aerospace and household appliances, the possibility of feeding from fossil and renewable fuels, the production of low environmental pollutants and the possibility of

* Corresponding author. Mechanical Engineering Department, College of Engineering, Najran University, Najran, Saudi Arabia
** Corresponding author. Department of Mechanical Engineering, Eastern Mediterranean University, Famagusta, TRNC, via, Mersin 10, Turkey.
E-mail addresses: jmmustafa@nu.edu.sa (J. Mustafa), hikmet.aybar@emu.edu.tr (H.Ş. Aybar).

https://doi.org/10.1016/j.csite.2023.103929
Received 11 July 2023; Received in revised form 5 December 2023; Accepted 16 December 2023
Available online 19 December 2023

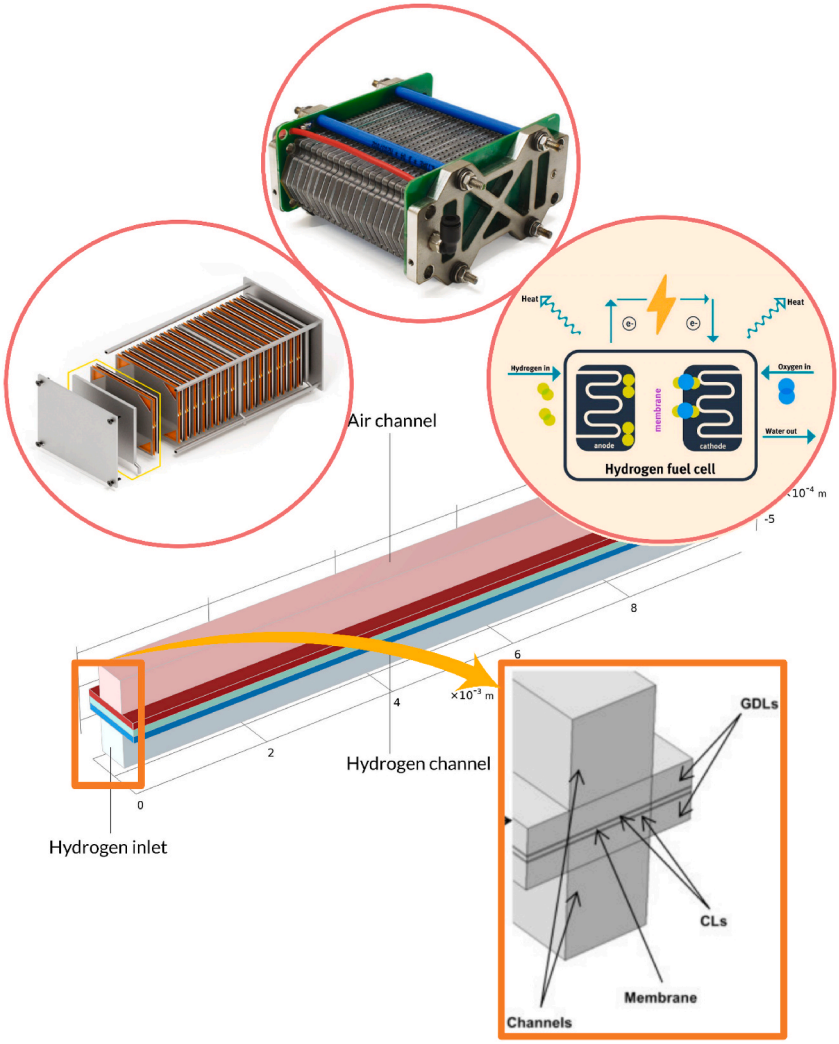

Fig. 1. A schematic of the polymer FUC.

simultaneous use of electrical and thermal energy [6]. FUCs are electrochemical devices that convert the chemical energy of the fuel into electricity directly. Unlike batteries, which are energy storage devices with limited reactants and limited operating time, the FUC produces electrical energy as long as they are fed with fuel and oxidizer [7]. In general, a FUC can be compared to an internal combustion engine in which the chemical energy of the fuel is directly used for electrical work without moving parts [8]. However, FUCs have many advantages over internal combustion engines. In the internal combustion engine, the energy conversion process is multi-stage and its value depends on the temperature of two hot and cold heat sources [9]. While a FUC is a constant temperature heat exchanger and does not have the limitations of Carnot law [10,11]. The absence of vibrations and noise, low maintenance cost, variety of fuel, the possibility of obtaining it such as hydrogen from renewable and non-renewable energy sources, and most importantly, low pollution can be considered as other advantages of FUCs [12,13].

In an experimental work, Freire et al. [14] evaluated the effect of operating parameters on the performance of a FUC by means of a spiral flow field with trapezoidal and rectangular cross-sections. The temperature of the cell, the pressure, and the wet temperature of the reactants had significant effects on the performance of the spiral field FUC with a trapezoidal cross section. The high water removal capability in this channel had a positive effect on the performance of the FUC when the produced water was high when the wet temperature of the reactants was higher than the temperature of the cell. On the other hand, when the amount of water was low, high water removal caused the humidity in the membrane to decrease. But, the influence of the wet temperature of the reactants was insignificant for the spiral channel with a rectangular cross-section. In an experimental work and 3D numerical simulations, Ferng and Lu [15] assessed the impact of flow patterns on the performance of a polymer FUC. The flow fields were parallel and spiral. The results demonstrated that spiral channels have a higher efficiency than parallel ones. The effect of channel depth was evaluated and it was found a significant effect on FUC performance when parallel channels were used but does not have much effect on FUC performance when spiral channels were utilized. Jang et al. [16] performed three-dimensional simulations of parallel, spiral, and z-type flow fields

Table 1
The source term parameters in Eq. (3).

H_2O	H_2	O_2
$\frac{i_v}{2F}$	$-\frac{i_v}{2F}$	$-\frac{i_v}{4F}$

numerical to assess their effect on fuel utilization, water transfer and FUC performance. In this study, velocity distribution, oxygen mass fraction, current density, water production amount, and pressure drop were estimated in detail. According to the results of this study, the spiral field had the best performance and the parallel field had the worst performance. The remarkable point was that an increment in the performance of the FUC in the spiral flow field and spiral type (z) leads to a higher pressure drop. Li et al. [17] determined the flow along the channel with a new design of bipolar plates with a suitable pressure drop and improved the removal of water from the FUC. In this design, liquid water outside the channel was observed in the cathode and anode during the experiments by neutron imaging techniques. Lu et al. [18] examined the geometry and orientation of the channel surface and water management in the polymer membrane FUC and found that if the direction of the channel is horizontal, the water flow moves in a spiral manner and as a result, non-uniform distribution of liquid water occurs. Hence, they employed the vertical channel.

Considering the mentioned importance of FUCs in the production and storage of energy in the future of human beings, a FUC is studied numerically in this article by changing the length of HOC for different voltages. Finally, the electrolyte potential (EPL), cell power (CPR), hydrogen mole fraction (HMF), water mole fraction (WMF), oxygen mole fraction (OMF), pressure, and rate changes in HOCs are analyzed by changing the effective variables.

2. Problem description

A three-dimensional polymer FUC is examined in this study. According to Fig. 1, the FUC consists of two channels in which hydrogen and oxygen flow and there are electrode layers and electrolyte cathode between them. Electrochemical reactions are carried out in the electrodes, and they are used for the simultaneous production of electricity and heat. In FUCs, the oxidation reaction of oxygen is one-third of oxidized hydrogen. In this paper, the performance of the FUC is evaluated by changing the voltage and its length.

The computational domain and the grid are shown in Fig. 1. The battery includes HOC and bipolar plates on the anode and cathode sides of the battery. The electrodes and membrane are located between the gas channels. In the current non-isothermal model, some simplifications are assumed: the gas mixture is assumed to be ideal, the gas penetration layer and the porous catalytic layer are homogeneous, and the flow is incompressible and laminar because the pressure and velocity gradients are small.

3. Governing equations and numerical method

Continuity and momentum equations are used to calculate pressure and velocity distribution. The continuity equation is [19,20]:

$$\rho\nabla.\vec{u} = Q_{br} \tag{1}$$

The value of the source term in Eq. (1) depends on the rate of the electrochemical reaction, which can be calculated as follows:

$$Q_{br} = \sum_m \sum_i R_{i,m} M_i \tag{2}$$

The rate of the electrochemical reaction is calculated as:

$$R_{i,m} = \frac{u_{i,m} i_v}{n_m F} \tag{3}$$

The source term parameters in Eq. (3) are presented in Table 1.
The momentum equation in a FUC channel is as follows:

$$\nabla.\left[-p + \frac{\mu}{\varepsilon_p}\left((\nabla\vec{u}) + (\nabla\vec{u})^T\right) - \frac{2\mu}{3\varepsilon_p}(\nabla\vec{u})\right] - \left(\frac{\mu}{K_{br}} + \frac{Q_{br}}{\varepsilon_p^2}\right)\vec{u} = 0 \tag{4}$$

By solving the mass transfer equation, the concentration distribution of species in the channel, gas diffusion layer and catalytic layer is obtained. The partial mass conservation equation of the species is as follows:

$$\nabla.\vec{j}_i + \rho(\vec{u}.\nabla)\omega_i = R_i \tag{5}$$

The Stefan-Maxwell equation is used to calculate the transfer flux of species:

$$\vec{j} = -\left(\rho\omega_i \sum_k D_{ik}^{eff}\left(\nabla x_k + \frac{1}{p_A}[(x_k - \omega_k)\nabla p_A]\right)\right) \tag{6}$$

The permeability coefficient at the operating temperature is calculated using Eq. (7) and the effective permeability coefficient is calculated using the Bergman equation Eq. 8 [20,21]:

Table 2
Comparison of voltage obtained from current changes in numerical simulations compared to experimental data [10].

Current density (A/m^2)	0.12	0.37	0.63	0.92	1.18	1.28
Joe et al. [10]	0.79	0.69	0.59	0.49	0.34	0.09
Present simulation	0.82	0.71	0.63	0.51	0.35	0.09
Error	3.8 %	2.9 %	6.8 %	4.0 %	2.9 %	0.0 %

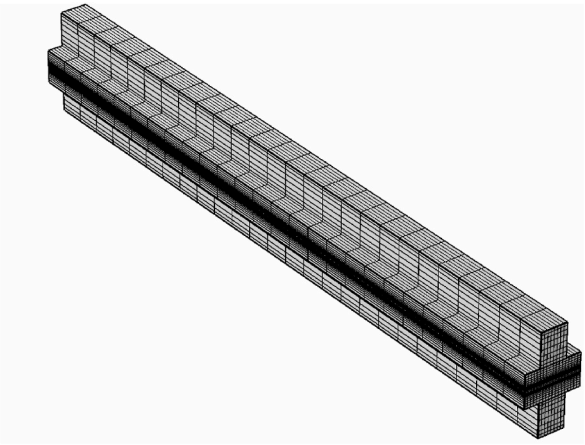

Fig. 2. A schematic of the 3D grid of the polymer FUC.

Table 3
Grid independence test (v = 0.05 V).

Elements number	630000	690000	765000	820000	890000	950000
Electrolyte potential (V)	0.049	0.061	0.073	0.078	0.079	0.079

$$D_{ik} = D_{ik-0}\left(\frac{T}{T_0}\right)^{1.5}\left(\frac{P_0}{P}\right) \tag{7}$$

$$D_{ik}^{eff} = \varepsilon^{1.5} D_{ik} \tag{8}$$

$$\rho = \frac{P_A M_n}{RT} \tag{9}$$

In multi-component mixtures, Fick's law is not accurate enough to determine the permeability flux, and the Stephen-Maxwell equation is used to determine the permeability flux in the mixtures. In the proton membrane exchange FUC, an electrochemical reaction occurs on the surface of the cathode and anode catalytic layers. To do this, the proton is transferred through the membrane, and the electrons that reach the cathode current pass through the external circuit. The electrical charge balance in the connectors on the anode and cathode sides is:

$$\nabla.\left(\sigma_s^{eff}\nabla\varnothing_s\right) = +\, i_{v,total} \tag{10}$$

$i_{v,total}$ is the current produced due to the electrochemical reaction on the catalytic layer (source term current). The electric charge balance on the membrane is as follows

$$\nabla.\left(\sigma_i^{eff}\nabla\varnothing_i\right) = -\, i_{v,total} \tag{11}$$

In the porous medium, the effective electrical conductivity of the electrode and the membrane is calculated using the Bergmann relation [22]:

$$\sigma_i^{eff} = \sigma_i \times \varepsilon_i^{1.5} \tag{12}$$

$$\sigma_s^{eff} = \sigma_s \times \varepsilon_s^{1.5} \tag{13}$$

The source term current is calculated utilizing the following equation. The linear relation of Butler-Volmer expresses charge current density. The kinetic equation of charge transfer is [23]:

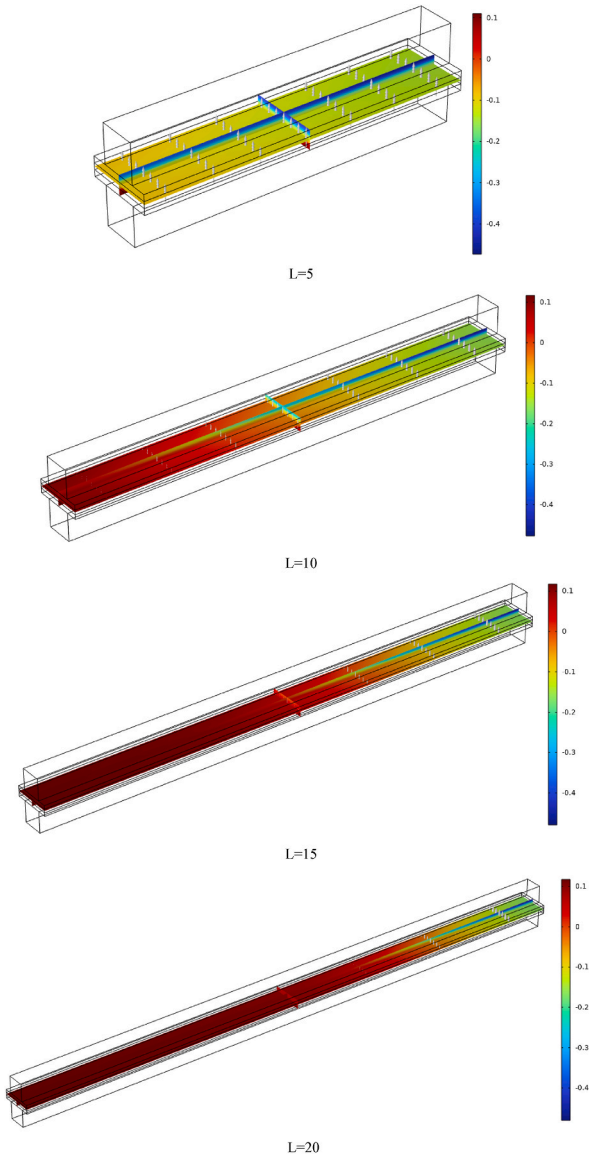

Fig. 3. EPL for different channel lengths of 5, 10, 15, and 20 when the voltage is 0.8 V.

$$i_a = i_{0,a}\left(\frac{Y_{H_2}}{Y_{H_2}^{ref}}\right)^{0.5}\left(\exp\left(\frac{\alpha_{a,a}F\eta_{act}}{RT}\right) - \exp\left(\frac{-\alpha_{a,c}F\eta_{act}}{RT}\right)\right) \tag{14}$$

The kinetics of cathode charge transfer is determined as follows:

$$i_c = i_{0,a}\left(\frac{Y_{o_2}}{Y_{o_2}^{ref}}\right)^{0.5}\left(\exp\left(\frac{\alpha_{a,a}F\eta_{act}}{RT}\right) - \exp\left(\frac{-\alpha_{a,c}F\eta_{act}}{RT}\right)\right) \tag{15}$$

During the chemical reaction, the driving force is the potential between the solid electric phase and the ion phase, which is known as the activation loss:

$$\eta = \varphi_s\varphi_i E_{eq} \tag{16}$$

The reversible potential is obtained using the following equation:

$$E_{eq} = 0.0025T + 0.2329 \tag{17}$$

The amount of average current density is equal to the total current density produced in the FUC divided by the surface of the

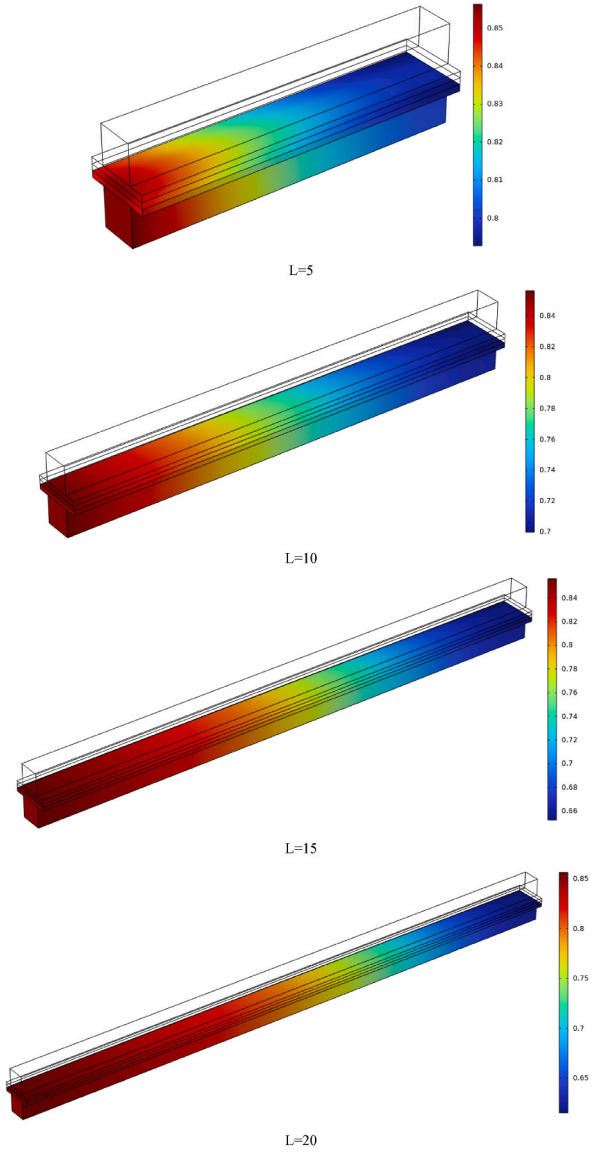

Fig. 4. HMF for different channel lengths of 5, 10, 15, and 20 when the voltage is 0.8 V.

geometry, which is calculated as [22]:

$$i_{ave} = \frac{1}{A}\int_{V_a} i_a dV = \frac{1}{A}\int_{V_c} i_c dV \tag{18}$$

4. Validation and grid study

To validate the FUC model, the comparison of voltage data with current change has been done. Operational parameters and dimensions for modeling are given in Ref. [10]. To compare the experimental data and the numerical data obtained from this research in Table 2, the battery voltage values are calculated with the current intensity. Table 2 shows the data obtained from the numerical modeling, which is in good agreement with the measured data in the study of Joe et al. [10] and shows an error of about 6.8 %. The output voltage from the FUC is obtained by subtracting the voltage losses from the theoretical voltage. Voltage losses are due to the activation energy, mass transfer, and ohmic loss.

This article aims to compare the FUC with the co-current gas flow in the channels as well as the FUC with counter-current gas flow. All geometric parameters and operating conditions are the same in both models. The computational grid structure is divided into 890000 cells after performing the grid independence test (Fig. 2). Table 3 demonstrates the result of the grid independence test. According to the result, the results do not change for the grid with 890000 cells and more, indicating that this grid can be selected for

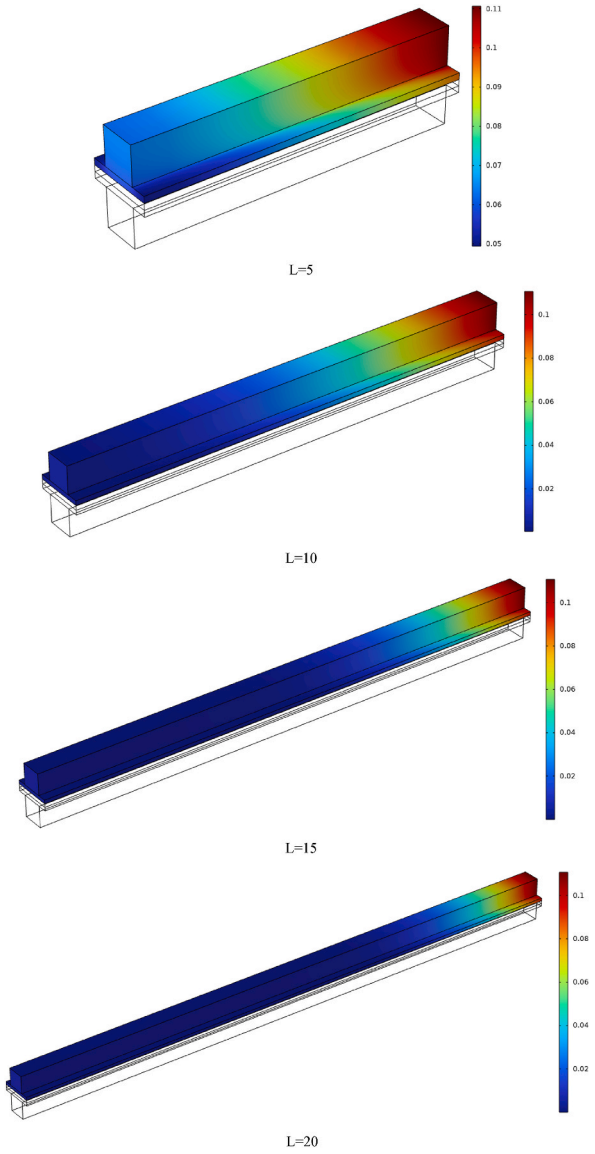

Fig. 5. OMF for different channel lengths of 5, 10, 15, and 20 when the voltage is 0.8 V.

the simulations to reduce the computational cost.

5. Results and discussion

Fig. 3 illustrates the EPL for different channel lengths of 5, 10, 15, and 20 mm when the voltage is 0.8 V. Electrolyte potential changes with increasing channel length in a fuel cell are significant because they affect the electrochemical processes inside the cell. Electrolyte potential represents the driving force for ion transport and reactions. The increase in length increases the resistance and leads to an increase in ohmic losses in the electrolyte. This causes it to disrupt the transport of ions through the electrolyte and affects the efficiency of electrochemical reactions. It can be observed that the amount of EPL is higher on the front side of the contours. The back side of the contours and the exit of the HOC have a lower EPL. Also, the amount of EPL is high at the bottom of the channel towards the hydrogen channel. This value is low on the upper side towards the oxygen channel. This issue can be seen especially when the length of HOCs is 5 mm. It causes the EPL changes to be higher. The changes in the EPL in the middle section along the length of the 5-mm channel are low, while its changes are high for the HOC length of 20 mm.

Fig. 4 depicts the HMF for different channel lengths of 5, 10, 15, and 20 when the voltage is 0.8 V. The amount of HMF entering the cathode channel is high. The amount of HMF is decreased along the length of the cathode channel by passing through the middle of the cathode channel and the electrochemical activities in the cell. It reaches the minimum value at the outlet of the channel. An increment in the length of the channel affects the HMF. It can be seen that increasing the length of the channel decreases the HMF at the outlet of

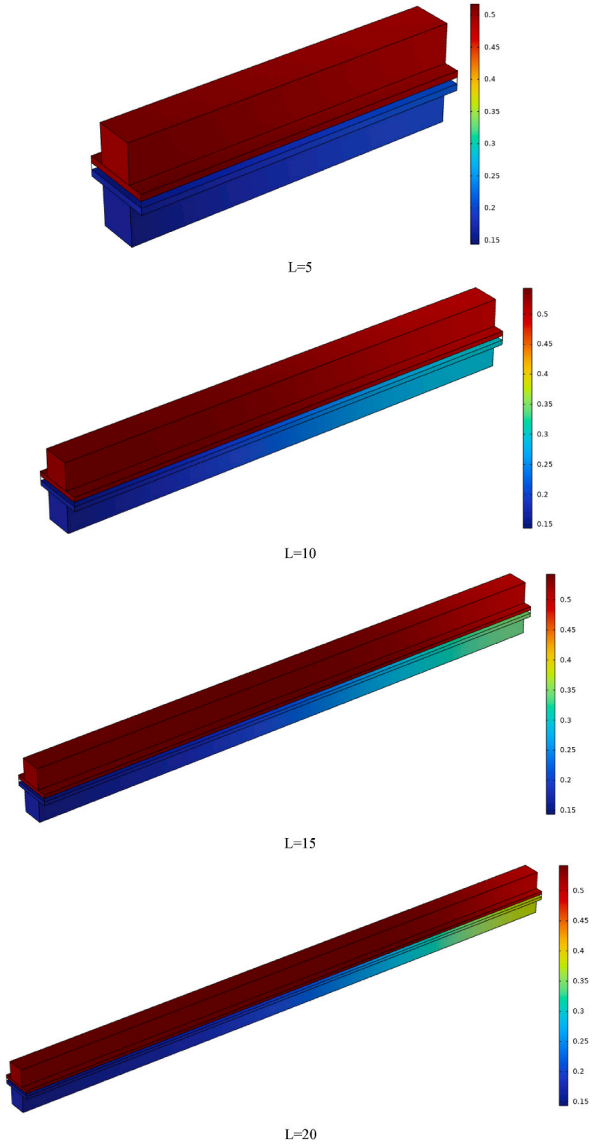

Fig. 6. WMF for different channel lengths of 5, 10, 15, and 20 when the voltage is 0.8 V.

the channel. If the channel has a longer length, hydrogen is exposed to more electrochemical activities, and as a result, the HMF at the outlet is reduced, which can cause less hydrogen loss. The minimum amount of HMF corresponds to the channel length of 20 mm, in which hydrogen is more exposed to electrochemical activities. On the other hand, when the channel length is 5 mm, the amount of HMF at the output is higher, because the hydrogen exits the channel faster, and as a result, it has a lower electrochemical activity.

Fig. 5 demonstrates the OMF for different channel lengths of 5, 10, 15, and 20 when the voltage is 0.8 V. The changes in the OMF depend on the channel length. It can be observed that the variation of the channel length changes the values of the OMF. Along the channel, the OMF is reduced due to oxygen consumption. The concentration of oxygen decreases from the inlet towards the catalyst, and it is low at the boundary of the catalyst. Most of the changes in the OMF occur in the initial parts of the channel, and little changes can be seen in the channel. Therefore, the excessive enhancement in the channel size does not affect the OMF, but it affects the OMF in the initial increases. It can be seen that the maximum and minimum amounts of OMF are changed with the change in the channel length.

Fig. 6 shows the WMF for different channel lengths of 5, 10, 15, and 20 when the voltage is 0.8 V. The WMF in the upper channel and in the oxygen channel is a little more than that in the hydrogen channel. Also, it is different along the length of each of these channels. In the beginning parts, the amount of WMF is low. Changes in the length of HOCs affect the WMF. Especially, changing the length of HOCs from 5 to 10 mm has a greater effect on the WMF. As the length of the HOCs is enhanced, oxygen and hydrogen can perform electrochemical activity for a longer time, and the mole fraction of water is also changed with the change in the length of the HOCs. For most of the lengths of the HOCs, the amount of WMF moves towards the average values for both channels at the end of the

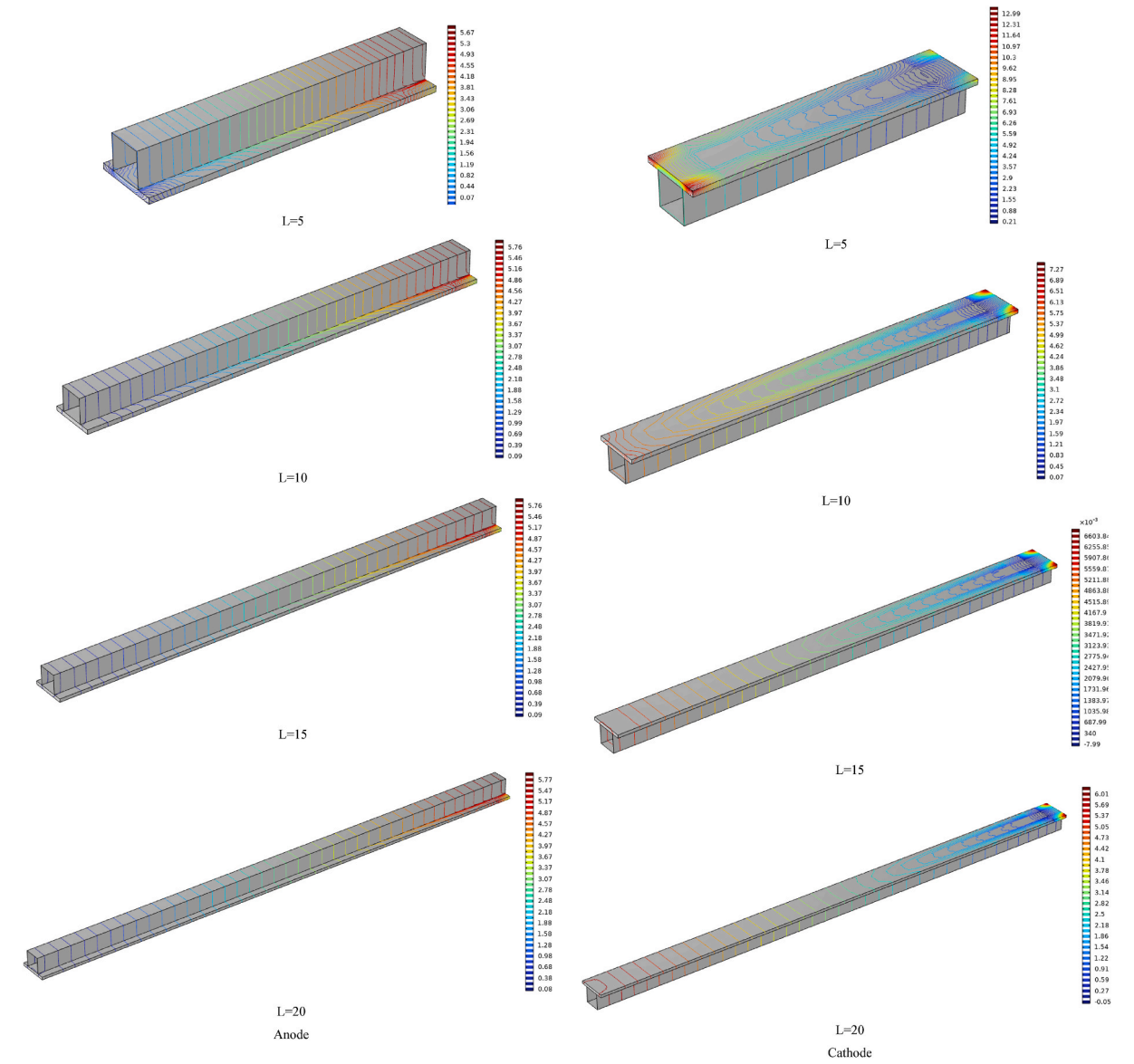

Fig. 7. Variations of pressure in HOC for different channel lengths of 5, 10, 15, and 20 when the voltage is 0.8 V.

channel.

Variations of pressure in HOC are illustrated in Fig. 7 for different channel lengths of 5, 10, 15, and 20 when the voltage is 0.8 V. Pressure changes in HOCs affect the amount of water, hydrogen, and OMF s. The pressure changes in the HOCs are due to the creation of a pressure gradient for the flow of oxygen and hydrogen in the anode and cathode channels. Since the pressure gradient in the HOCs is constant, the velocity changes in them by increasing the length of the channels, which leads to a change in the flow rate of hydrogen and oxygen in the anode and cathode channels. According to previous studies [16,24], increasing the length of fuel cell channels has increased the pressure drop. The pressure changes in the HOCs are similar to each other, and the small differences in them are due to the different properties of these two gases, which slightly affected the shear stress. Maximum pressure changes occur at the end of the channels and at the channel outlet, when the fluid leaves the HOCs. The shear stress along the hydrogen and oxygen fuel cell walls causes friction between the gas and the wall surface. This friction creates a drag force, disrupting the gas flow and resulting in lower velocities near the walls. Due to the shear stress on the walls, the velocity on the side of the walls has been affected by the velocity of the wall, which was zero. On the walls, the principle of non-slip has been used, and as a result, the speed on the walls has tended to zero. Based on the momentum equations solved on the walls and Newtonian fluid are considered and their relationships, the fluid velocity in different sections of the channels is also influenced by the wall velocity of the channel. The importance lies in the effect on mass transfer and reaction rate. Slowing down the walls can prevent effective gas diffusion and contact with the catalyst and affect the overall electrochemical reactions.

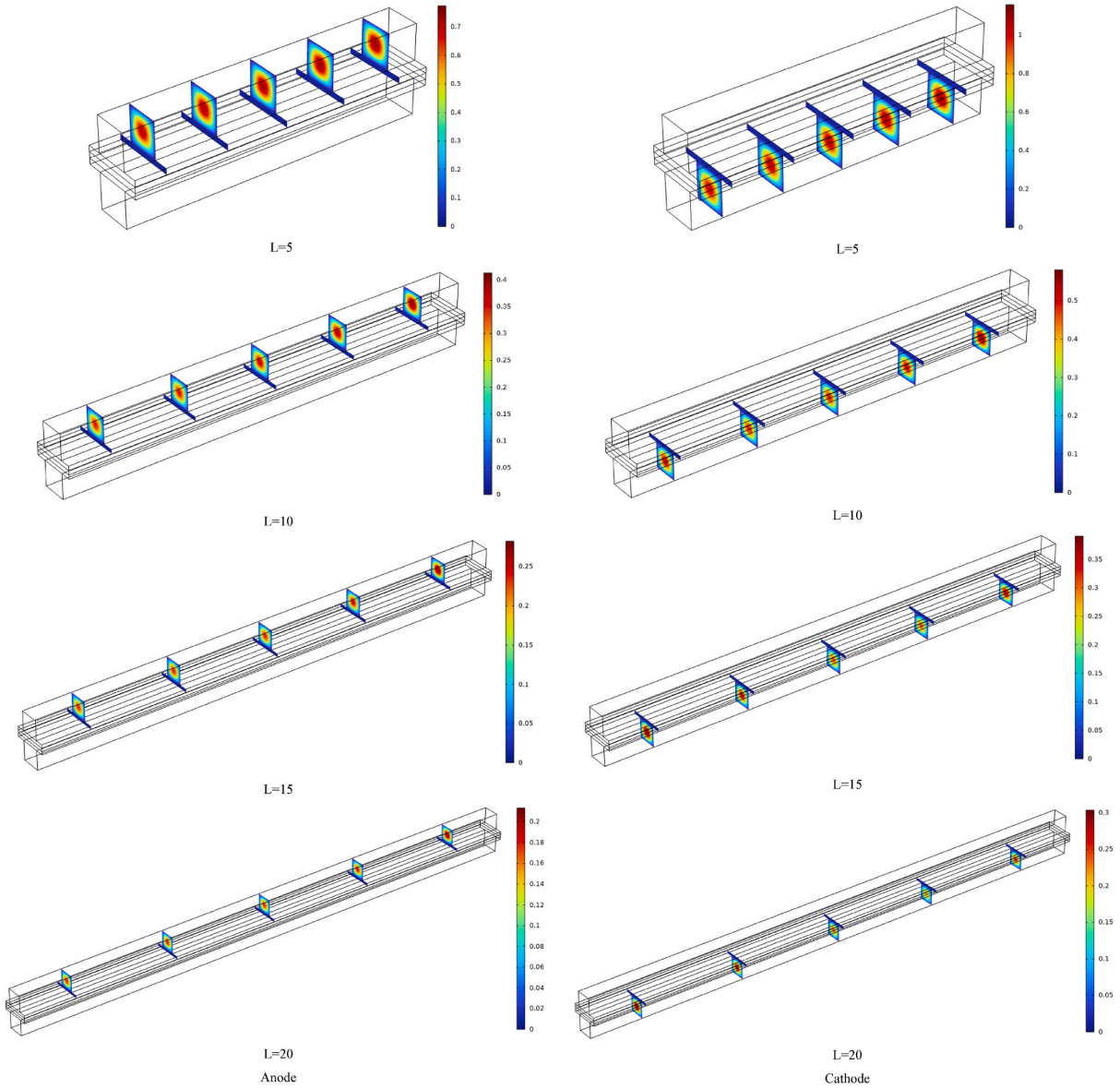

Fig. 8. Variations of velocity in HOC for different channel lengths of 5, 10, 15, and 20 when the voltage is 0.8 V.

Variations of velocity in HOC are depicted in Fig. 8 for different channel lengths of 5, 10, 15, and 20 when the voltage is 0.8 V. The velocity values of oxygen and hydrogen gases in the anode and cathode channels depend on the pressure gradient in them. Since the inlet and outlet pressure in the HOCs is constant, the velocity values in the HOCs by changing the length of the HOCs. On the sides of the walls of the HOCs, the gas velocity values are very low due to the shear stress on the walls. On the other hand, in the middle of the HOCs, the velocity values are maximal. As seen in the obtained results, speed changes along the HOC channel affect its performance. In fact, according to the obtained results, speed changes and choosing the optimal speed can guarantee the transfer of the effective mass of the reactants to the catalyst surfaces and cause effective electrochemical reactions. On the other hand, too low a speed leads to an incomplete reaction and reduces the yield, while too high a speed may hinder the transfer of the reactant. Balancing these factors is critical to maximizing fuel cell efficiency and overall performance. So the changes along the HOCs have more impact on the maximum velocity. Therefore, the values of the maximum velocity in the HOCs are decreased with the length of the channel, so that the highest maximum velocity corresponds to the channel length of 5 mm, and the lowest maximum velocity corresponds to the channel length of 20 mm, Changes in the velocity in the channel are also important in terms of the flow rate and the amount of power to move the gases.

Fig. 9 shows the average mole fraction of hydrogen for different voltages and various channel lengths of 5, 10, 15, and 20 mm. According to the study of Ahmadi and Rostami [25], it can be seen that the average mole fraction of hydrogen decreases with increasing channel length. As the voltage is enhanced, the average mole fraction of hydrogen is decreased for different lengths of HOC. The consumption of hydrogen is increased with the voltage, and as a result, the amount of HMF is reduced. Therefore, the amount of

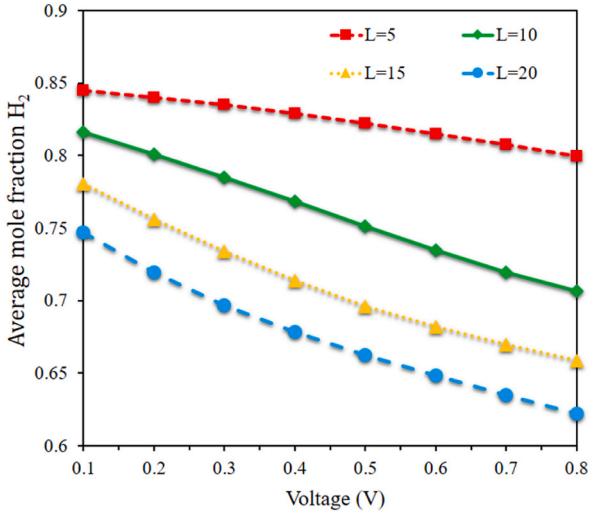

Fig. 9. Average mole fraction of hydrogen for different voltages and various channel lengths of 5, 10, 15, and 20 mm.

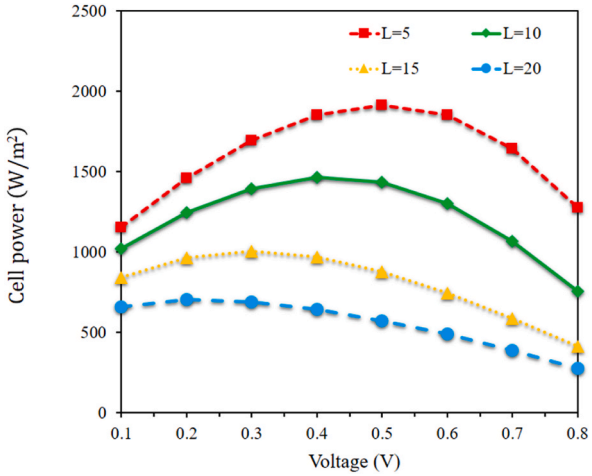

Fig. 10. CPR variations for different voltages and various channel lengths of 5, 10, 15, and 20 mm.

hydrogen loss is lower at higher voltages. The increase in the length of the HOC reduces the amount of the HMF. Using channels with a longer length intensifies the consumption of hydrogen in the FUC; thus, there is a decrease in the quantity of hydrogen loss.. The minimum amount of HMF corresponds to the channel length of 20 mm and the voltage of 0.8 V, while the maximum amount of HMF corresponds to the channel length of 5 mm and the voltage of 0.1 V. The decrease in the amount of HMF with the voltage is more significant for the higher channel lengths. In the higher channel lengths, the consumption of hydrogen is increased with the voltage, and as a result, the amount of HMF is reduced.

Fig. 10 illustrates the CPR variations for different voltages and various channel lengths of 5, 10, 15, and 20 mm. Changes in the voltage lead to parabolic changes in the CPR in such a way that the CPR in the HOC first enhances and then reduces with the voltage. In shorter channels, the rise in voltage results in a larger enhancement in the CPR. In higher channel lengths, the amount of increase in CPR is less, and a more decreasing trend in CPR can be seen with the voltage. Enhancing the length of the channel reduces CPR. An increment in the length of the HOC, especially from 5 to 10 mm, reduces the CPR. The maximum amount of CPR corresponds to the channel length of 5 mm and a voltage of 0.5 V, while the minimum CPR corresponds to the channel length of 20 mm and a voltage of 0.8 V. When the HOC length is 5 mm, the amount of CPR at the voltage of 0.1 V is lower than that at a voltage of 0.8 V. For other lengths of HOC, the amount of CPR at a voltage 0.8 V is less than that at the voltage of 0.1 V. For other lengths of HOC, the amount of CPR at a voltage 0.8 V is less than that at the voltage of 0.1 V. In a fuel cell in general, the channels may be faster to carry out the transfer and accelerate the electrochemical reactions. But increasing the length reduces the power of the fuel cell. In the channels, the speed increases, which provides the transfer of various materials and improves the electrochemical reactions. While in the long term, the rate of pressure increase has increased due to the more uniform presence, thus increasing the transfer of mass potential and subsequently reducing the output. But in changing the voltage of the fuel cell at the beginning with increasing voltage, the output power may

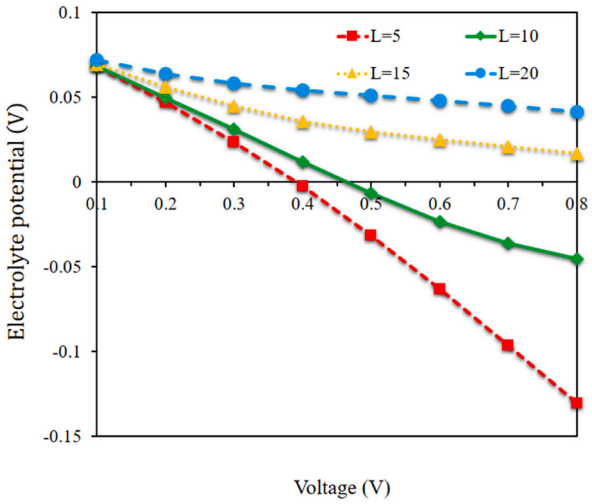

Fig. 11. EPL variations for different voltages and various channel lengths of 5, 10, 15, and 20 mm.

increase due to excessive reduction of activation. The highest voltage causes faster electrochemical reactions at the electrodes and increases the output power. As the voltage increases, the mass transfer overpotential may become dominant. A higher voltage can create limitations in the diffusion and transport of the reactant and reduce the output power despite the high voltage. An optimal point can be seen in the diagram, which has the maximum power of the fuel cell at the optimal point, which results in the reduction of the excess activation potential with losses caused by the increase in excess potential, mass transfer, and can lead to an increase in output power.

Fig. 11 demonstrates the EPL variations for different voltages and various channel lengths of 5, 10, 15, and 20 mm. An enhancement in the voltage greatly reduces the EPL. This decrease is greater for smaller lengths of the HOC. An increment in the length of HOC enhances the amount of EPL, which is more significant for higher voltages. When the voltages are higher, using longer channels enhances the EPL. The highest quantity of EPL is related to a voltage of 0.1 V and a channel length of 20 mm. The minimum value of the EPL corresponds to the channel length of 5 mm and a voltage of 0.8 V.

6. Conclusions

This article presents the simulation of a FUC using COMSOL software. The outputs of the FUC, including EPL, CPR, HMF, WMF, OMF, pressure and velocity changes in HOCs, etc. are determined by changing the length of the channels in the FUC in the range of 5–20 mm and altering the voltage from 0.1 to 0.8 V. Longer channels may increase the residence time of the reactants, potentially increasing the reaction rate. However, too many channels may cause more pressure drop and inefficiency. Understanding how these geometrical parameters affect the efficiency and output power is very important for the design of high-performance fuel cells, so in this review, according to the discussed results, it can be pointed out that:

1 According to the pressure gradient in the HOCs, an increment in the length of the channels reduces the maximum velocity in the HOCs.
2 An enhancement in the voltage significantly diminishes the amount of EPL, while intensifying the length of the HOC enhances the EPL.
3 At higher voltages, the use of longer channels intensifies the EPL.
4 The maximum amount of CPR is related to the channel length of 5 mm and a voltage of 0.5 V.
5 Enhancing the length of HOC reduces the amount of CPR.
6 An increment in the length of the channel and voltage reduces the mole fraction of hydrogen. Increasing the voltage has a more significant reduction in mole fraction of hydrogen when the length of the HOC is smaller.
7 As the FUC length increases, the EPL difference in the beginning and end of the channel increases. On the other hand, HMF decreases with increasing fuel cell length. The longer the length, the more the amount of hydrogen exposed to electrochemical activities, and as a result, the amount of HMF in outlet was also lower. Increasing the size of the same channel does not have a great effect on OMF, but it has an effect on the amount of OMF in increasing its initial changes. As the volume increases, the WMF also increases.

CRediT authorship contribution statement

Jawed Mustafa: Data curation, Investigation, Project administration, Writing – original draft, Writing – review & editing. **Saeed Alqaed:** Methodology, Writing – review & editing. **S. Mohammad Sajadi:** Investigation, Project administration, Writing – review & editing. **Hikmet Ş. Aybar:** Data curation, Methodology, Writing – original draft, Writing – review & editing.

Declaration of competing interest

The authors declare that they have no known competing financial interests or personal relationships that could have appeared to influence the work reported in this paper.

Data availability

No data was used for the research described in the article.

Acknowledgements

The authors are thankful to the Deanship of Scientific Research at Najran University for funding this work, under the Distinguish Research Funding Program grant code (NU/DRP/SERC/12/18).

References

[1] M.W. Azam, G.Q. Chaudhary, U. Sajjad, N. Abbas, W.-M. Yan, Performance investigation of solar assisted desiccant integrated Maisotsenko cycle cooler in subtropical climate conditions, Case Stud. Therm. Eng. 44 (2023), 102864.
[2] U. Sajjad, M. Amer, H.M. Ali, A. Dahiya, N. Abbas, Cost effective cooling of photovoltaic modules to improve efficiency, Case Stud. Therm. Eng. 14 (2019), 100420.
[3] A. Ali, M.A. Khan, N. Abbas, H. Choi, Prediction of hydrogen storage in dibenzyltoluene empowered with machine learning, J. Energy Storage 55 (2022), 105844.
[4] F. Guo, C. Li, H. Liu, K. Cheng, J. Qin, Matching and performance analysis of a solid oxide fuel cell turbine-less hybrid electric propulsion system on aircraft, Energy 263 (2023), 125655.
[5] T. Eisa, M.A. Abdelkareem, D.A. Jadhav, H.O. Mohamed, E.T. Sayed, A.G. Olabi, P. Castaño, K.-J. Chae, Critical review on the synthesis, characterization, and application of highly efficient metal chalcogenide catalysts for fuel cells, Prog. Energy Combust. Sci. 94 (2023), 101044.
[6] N.H. Park, J. Kim, Y. Ahn, Fabric-based self-pumping, single-stream microfluidic fuel cell, Electrochim. Acta 446 (2023), 142106.
[7] J.M. Haan, J.R. Ragadi, K. Hohl, L. Hernandez, J.L. Haan, High performance direct liquid fuel cells powered by xylose or glucose, Int. J. Hydrogen Energy (2023).
[8] A. Choudhury, H. Chandra, A. Arora, Application of solid oxide fuel cell technology for power generation—a review, Renew. Sustain. Energy Rev. 20 (2013) 430–442.
[9] V. Patil, P.V. Reshmi, S. Prajna, Yashaswini Yashaswi, D. Haleshappa, A. Jayarama, R. Pinto, Degradation mechanisms in PEM fuel cells: a brief review, Mater. Today: Proc. (2023).
[10] H. Ju, H. Meng, C.-Y. Wang, A single-phase, non-isothermal model for PEM fuel cells, Int. J. Heat Mass Tran. 48 (2005) 1303–1315.
[11] V. Mehta, J.S. Cooper, Review and analysis of PEM fuel cell design and manufacturing, J. Power Sources 114 (2003) 32–53.
[12] S. Gupta, A. Patro, Y. Mittal, S. Dwivedi, P. Saket, R. Panja, T. Saeed, F. Martínez, A.K. Yadav, The race between classical microbial fuel cells, sediment-microbial fuel cells, plant-microbial fuel cells, and constructed wetlands-microbial fuel cells: applications and technology readiness level, Sci. Total Environ. 879 (2023), 162757.
[13] A. Kasaeian, M. Javidmehr, M.R. Mirzaie, L. Fereidooni, Integration of solid oxide fuel cells with solar energy systems: a review, Appl. Therm. Eng. 224 (2023), 120117.
[14] L.S. Freire, E. Antolini, M. Linardi, E.I. Santiago, R.R. Passos, Influence of operational parameters on the performance of PEMFCs with serpentine flow field channels having different (rectangular and trapezoidal) cross-section shape, Int. J. Hydrogen Energy 39 (2014) 12052–12060.
[15] Y.-M. Ferng, A. Su, S.-M. Lu, Experiment and simulation investigations for effects of flow channel patterns on the PEMFC performance, Int. J. Energy Res. 32 (2008) 12–23.
[16] J.-H. Jang, W.-M. Yan, H.-Y. Li, W.-C. Tsai, Three-dimensional numerical study on cell performance and transport phenomena of PEM fuel cells with conventional flow fields, Int. J. Hydrogen Energy 33 (2008) 156–164.
[17] X. Li, I. Sabir, J. Park, A flow channel design procedure for PEM fuel cells with effective water removal, J. Power Sources 163 (2007) 933–942.
[18] Z. Lu, C. Rath, G. Zhang, S.G. Kandlikar, Water management studies in PEM fuel cells, part IV: effects of channel surface wettability, geometry and orientation on the two-phase flow in parallel gas channels, Int. J. Hydrogen Energy 36 (2011) 9864–9875.
[19] C.-Y. Wang, Fundamental models for fuel cell engineering, Chem. Rev. 104 (2004) 4727–4766.
[20] R. O'hayre, S.-W. Cha, W. Colella, F.B. Prinz, Fuel Cell Fundamentals, John Wiley & Sons, 2016.
[21] B. Wesrb, E. Lightfoot, John Wiley and Sons, Inc, Transport Phenomena, New York, 1960.
[22] F. Barbir, PEM Fuel Cells: Theory and Practice, Academic press, 2012.
[23] N. Siegel, M. Ellis, D. Nelson, M. Von Spakovsky, A two-dimensional computational model of a PEMFC with liquid water transport, J. Power Sources 128 (2004) 173–184.
[24] A.P. Manso, F.F. Marzo, J. Barranco, X. Garikano, M. Garmendia Mujika, Influence of geometric parameters of the flow fields on the performance of a PEM fuel cell. A review, Int. J. Hydrogen Energy 37 (2012) 15256–15287.
[25] N. Ahmadi, S. Rostami, Enhancing the performance of polymer electrolyte membrane fuel cell by optimizing the operating parameter, J. Braz. Soc. Mech. Sci. Eng. 41 (2019) 220.